Chronic epithelial NF-κB activation accelerates APC loss and intestinal tumor initiation through iNOS up-regulation

Helena Shaked[a], Lorne J. Hofseth[b], Alena Chumanevich[b], Alexander A. Chumanevich[b], Jin Wang[c], Yinsheng Wang[c], Koji Taniguchi[a,d], Monica Guma[a], Steve Shenouda[e], Hans Clevers[f], Curtis C. Harris[g], and Michael Karin[a,1]

[a]Department of Pharmacology and [e]Laboratory of Mucosal Immunity and the William K. Warren Medical Research Center for Celiac Disease, School of Medicine, University of California at San Diego, La Jolla, CA 92093; [b]Department of Pharmaceutical and Biomedical Sciences, South Carolina College of Pharmacy, University of South Carolina, Columbia, SC 29208; [c]Department of Chemistry, University of California, Riverside, CA 92521; [d]Department of Microbiology and Immunology, Keio University School of Medicine, Tokyo 160-8582, Japan; [f]Hubrecht Institute for Developmental Biology and Stem Cell Research, 3584 CT, Utrecht, The Netherlands; and [g]Laboratory of Human Carcinogenesis, National Cancer Institute, National Institutes of Health, Bethesda, MD 20892

Contributed by Michael Karin, July 12, 2012 (sent for review June 14, 2012)

The role of NF-κB activation in tumor initiation has not been thoroughly investigated. We generated *Ikkβ(EE)*^{IEC} transgenic mice expressing constitutively active IκB kinase β (IKKβ) in intestinal epithelial cells (IECs). Despite absence of destructive colonic inflammation, *Ikkβ(EE)*^{IEC} mice developed intestinal tumors after a long latency. However, when crossed to mice with IEC-specific allelic deletion of the adenomatous polyposis coli (*Apc*) tumor suppressor locus, *Ikkβ(EE)*^{IEC} mice exhibited more β-catenin^{+} early lesions and visible small intestinal and colonic tumors relative to *Apc*$^{+/\Delta IEC}$ mice, and their survival was severely compromised. IEC of *Ikkβ(EE)*^{IEC} mice expressed high amounts of inducible nitric oxide synthase (iNOS) and elevated DNA damage markers and contained more oxidative DNA lesions. Treatment of *Ikkβ(EE)*^{IEC}/*Apc*$^{+/\Delta IEC}$ mice with an iNOS inhibitor decreased DNA damage markers and reduced early β-catenin^{+} lesions and tumor load. The results suggest that persistent NF-κB activation in IEC may accelerate loss of heterozygocity by enhancing nitrosative DNA damage.

Colorectal cancer (CRC) is one of the most common cancers worldwide affecting 5% of Americans, nearly one-third of whom will die from the disease (1). Patients with inflammatory bowel disease (IBD), such as ulcerative colitis, are more likely to develop CRC (2), underscoring the well-established link between chronic inflammation and cancer (3). Genetic and functional analyses of mouse models of inflammation-dependent cancer, including colitis-associated CRC (CAC), have shown that inflammation mainly acts as a tumor promoter (4, 5). Nonetheless, in certain colitis models in mice, inflammation alone suffices for tumor development (6–8) and recent studies have suggested that inflammation-induced DNA damage can link between chronic colitis and tumor initiation (9, 10). These findings are consistent with observations of oxidative DNA damage and increased p53 mutation load in the mucosa of ulcerative colitis patients (11, 12).

CRC can be caused by germ-line mutations in the adenomatous polyposis coli (*APC*) tumor suppressor gene, a hallmark of the familial adenomatous polyposis (FAP) syndrome, which accounts for 0.2% of all CRC cases (13). APC loss of function is a tumor-initiating event in sporadic cancer as well (14), and in both cases mutations frequently involve allelic loss of *APC* (15). Loss of APC function results in activation of β-catenin signaling, the first step in the oncogenic pathway that leads to CRC development (16). Nonsteroidal antiinflammatory drugs (NSAIDs) can reduce the risk of sporadic CRC and FAP-induced CRC (17–19), suggesting that inflammatory processes may contribute to intestinal tumorigenesis also in the absence of preexisting clinical inflammation. In mouse models of CRC induced by *APC* loss of function, inhibition of two major enzymes responsible for the generation of secondary inflammatory mediators, cyclooxygenase 2 (Cox2) and inducible nitric oxide synthase (iNOS), or genetic ablation of their respective genes, suppress tumor formation (20, 21). Also, experimental colitis was shown to increase tumorigenesis in *Apc*$^{+/Min}$ mice through an iNOS-dependent mechanism (22).

The major role of iNOS, when expressed in phagocytic cells upon activation of NF-κB and other transcription factors, is to fight pathogens during infection by catalyzing the production of toxic reactive nitrogen species (RNS) (23). However, iNOS has also been implicated in the pathogenesis of IBD, where it is expressed in intestinal epithelial cells (IECs) and contributes to tissue damage (24, 25). iNOS is also expressed at physiological levels by IECs in the distal portion of the small intestine (SI) (26). In *Apc*$^{+/Min}$ mice, inhibition of nitric oxide radical (NO•) production or *Nos2* gene ablation were shown to significantly reduce the number of intestinal polyps, but the mechanism by which iNOS contributes to polyp formation remains unraveled (21). For instance, it is not clear whether iNOS expression promotes inflammation or whether it leads to direct DNA damage in IECs, in vivo.

NF-κB is a transcription factor regulating immune and inflammatory responses that also has an important role in tumorigenesis, especially in inflammation-driven cancers (27). NF-κB is expressed in many types of cancer and was shown to link inflammation to cancer development (3, 28). Previously, we found that NF-κB activation in both IECs and lamina propria macrophages plays a critical role in the development of CAC (4). In IECs, the protumorigenic function of NF-κB appears to be mediated through its antiapoptotic effect that prevents the elimination of premalignant cells, in which β-catenin signaling has been activated due to mutations in the *Catnb* gene. Thus, in this model NF-κB acts as a tumor promoter (4). More recently, IEC-specific transgenic activation of IKKβ, a protein kinase that plays a critical role in NF-κB activation (29), was shown to lead to development of intestinal adenomas in older mice (30), but the mechanisms through which IKKβ activation promoted the development of such tumors were not fully described.

To further study the effect of chronic NF-κB activation in IECs on tumor development, we used *Ikkβ(EE)*^{IEC} mice that express constitutively active IKKβ [IKKβ(EE)] from the IEC-specific *Villin* promoter (31). Although IKKβ activation led to development of spontaneous intestinal tumors, this process was slow and inefficient. We therefore crossed *Ikkβ(EE)*^{IEC} mice with *Apc*$^{+/F}$/*Villin-Cre* mice and found that IKKβ(EE) expression strongly enhanced tumor development caused by allelic loss of *Apc*. This effect was exerted very early in the tumorigenic

Author contributions: H.S., L.J.H., Y.W., C.C.H., and M.K. designed research; H.S., L.J.H., A.C., A.A.C., J.W., K.T., M.G., S.S., and H.C. performed research; L.J.H., Y.W., and M.G. contributed new reagents/analytic tools; H.S., L.J.H., A.C., A.A.C., J.W., Y.W., and H.C. analyzed data; and H.S. and M.K. wrote the paper.

The authors declare no conflict of interest.

[1]To whom correspondence should be addressed. E-mail: karinoffice@ucsd.edu.

This article contains supporting information online at www.pnas.org/lookup/suppl/doi:10.1073/pnas.1211509109/-/DCSupplemental.

CELL BIOLOGY

pathway and is likely to be mediated through an apoptosis-independent mechanism that involves iNOS. Up-regulated iNOS expression in *Ikkβ(EE)*^{IEC} mice causes constitutive nitrosative stress and DNA damage, thereby accelerating tumor initiation due to *Apc* loss of heterozygocity (LOH).

Results

Expression of IKKβ(EE) in IECs Induces Tumorigenesis After a Long Latency. To explore effects of chronic NF-κB activation in IECs, we generated *Ikkβ(EE)*^{IEC} transgenic mice (31). These mice express constitutively active IKKβ(EE) from the *Villin* promoter and display NF-κB activation in IECs of their SI and colon and up-regulation of numerous NF-κB target genes (31). Although the SI of *Ikkβ(EE)*^{IEC} mice is hyperplastic (31), the mice rarely exhibit spontaneous gastrointestinal tumors before 1 y of age. However, spontaneous tumors in the duodenum were detected in 10 out of 10 one-year-old mice (Fig. S1*A*). Histological analysis indicated that these tumors were adenomas (Fig. S1*B*). Curiously, none of these tumors exhibited nuclear β-catenin staining (Fig. S1*B*). Immunoblot and IHC analysis revealed elevated expression of p53 (Fig. S1 *C* and *E*), but RT-PCR analysis showed no up-regulation of p53 target genes (Fig. S1*D*). In fact, most p53 targets, as well as the β-catenin target Lgr5, were down-regulated, whereas expression of c-Myc and Sox9, two transcription factors involved in tumorigenesis and adult stem cell maintenance (32–35), was up-regulated (Fig. S1 *D* and *E*). We therefore speculated that p53 might have been inactivated in aged *Ikkβ(EE)*^{IEC} mice. Moreover, we analyzed 10- to 12-mo-old mice with IEC-specific deletion of p53 [*p53*$^{F/F}$*/Villin-Cre* and *p53*$^{F/F}$*/Villin-Cre/Ikkβ(EE)*^{IEC}] and found duodenal tumors in roughly 50% of them, regardless of the presence of the *Ikkβ(EE)* transgene (data not shown). This finding supports the notion that p53 loss of function may contribute to tumorigenesis in aged *Ikkβ(EE)*^{IEC} mice.

Expression of IKKβ(EE) in IECs Accelerates Tumorigenesis in *Apc*$^{+/\Delta IEC}$ Mice. The absence of nuclear β-catenin in spontaneous adenomas was perplexing because previous studies have shown that inflammation-driven NF-κB activation in IECs potentiates tumorigenesis initiated by the chemical procarcinogen azoxymethane (AOM), which induces activating mutations in the *Catnb* gene resulting in nuclear β-catenin accumulation (4). Furthermore, the long latency associated with formation of spontaneous tumors made it difficult to understand whether and how NF-κB affects tumor initiation. We therefore decided to test whether NF-κB activation in IECs can accelerate tumorigenesis caused by *Apc* loss. To this end, we crossed *Ikkβ(EE)*^{IEC} mice with *Apc*$^{+/F}$*/Villin-Cre* mice, in which one *Apc* allele is deleted in IECs that express Villin-driven Cre recombinase (36). *Apc*$^{+/F}$/Villin-Cre mice, herein referred to as *Apc*$^{+/\Delta IEC}$ mice, develop SI and colonic adenomas before 7 mo of age, upon loss of the wild type (WT) *Apc* allele (36). We found that in *Ikkβ(EE)*^{IEC}*/Apc*$^{+/\Delta IEC}$ hybrids, tumor development was highly accelerated relative to *Apc*$^{+/\Delta IEC}$ mice. Most of the hybrid mice started losing weight at 10 wk of age and died shortly after 3 mo of age, whereas most of their *Apc*$^{\Delta IEC/+}$ counterparts survived more than 5 mo (Fig. 1*A*). Three-month-old *Ikkβ(EE)*^{IEC}*/Apc*$^{+/\Delta IEC}$ mice displayed multiple tumors in the proximal SI and the colon (Fig. 1*B* and Fig. S2*A*), and colonic tumors were slightly larger in these mice than in *Apc*$^{+/\Delta IEC}$ mice (Fig. S2*B*). Correspondingly, average tumor load, a sum of all tumor diameters in a given mouse (37), was significantly higher in the SI and colon of *Ikkβ(EE)*^{IEC}*/Apc*$^{+/\Delta IEC}$ mice than in *Apc*$^{+/\Delta IEC}$ mice (Fig. 1*B*). All of the observed tumors were adenomas that displayed β-catenin activation and no obvious strain-specific differences in tumor histology were noted (Fig. 1*C*). Genomic DNA analysis showed loss of the WT *Apc* allele in colonic tumors of both strains (Fig. S2*C*).

Because the *Ikkβ(EE)* transgene appeared to mostly increase tumor number and not size, we speculated that it might accelerate either tumor initiation or early establishment. Thus, we analyzed histological sections from the proximal SI and colons of

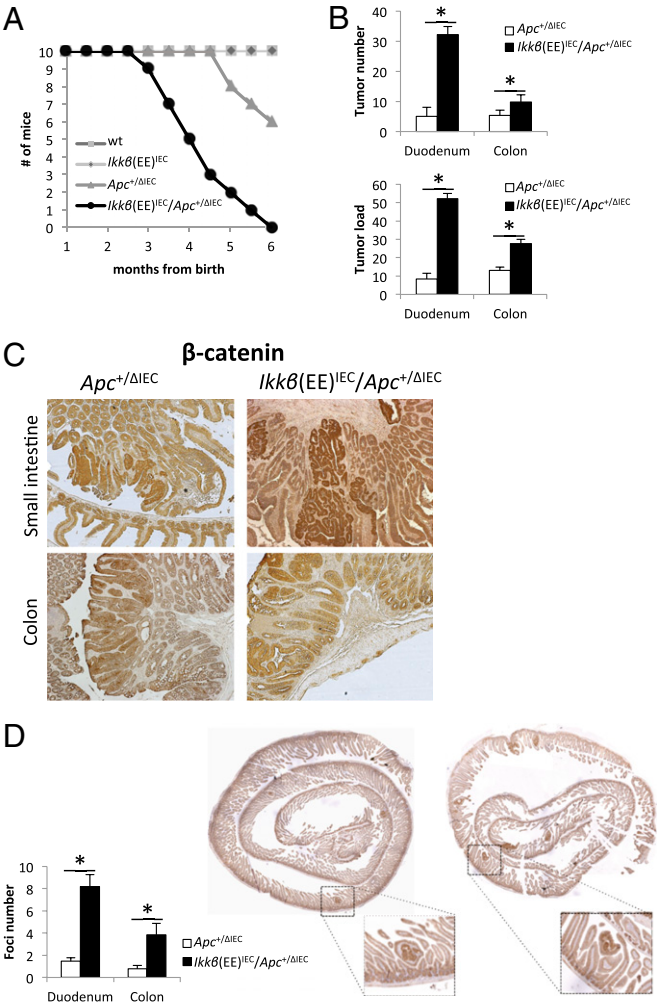

Fig. 1. Increased tumorigenesis in *Ikkβ(EE)*^{IEC}*/Apc*$^{+/\Delta IEC}$ mice. (*A*) Survival rates of the indicated strains of mice. (*B*) Tumor numbers and tumor load (the sum of tumor diameters) in the proximal SI (proximal 6 cm, herein referred as duodenum) and colon of *Ikkβ(EE)*^{IEC}*/Apc*$^{+/\Delta IEC}$ and *Apc*$^{+/\Delta IEC}$ mice. (*C*) IHC for β-catenin performed on paraffin sections of tumors from 3-mo-old mice of the indicated genotypes. (*D*) IHC for β-catenin performed on "Swiss-roll" preparations of 1-mo-old mice of the indicated genotypes. Bar graphs show the numbers of β-catenin$^+$ foci in 4- to 6-wk-old mice.

4- to 6-wk-old *Ikkβ(EE)*^{IEC}*/Apc*$^{+/\Delta IEC}$ and *Apc*$^{+/\Delta IEC}$ mice by β-catenin staining. We observed a large increase in the number of nuclear β-catenin$^+$ foci in *Ikkβ(EE)*^{IEC}*/Apc*$^{+/\Delta IEC}$ mice relative to *Apc*$^{+/\Delta IEC}$ mice (Fig. 1*D*). Collectively, these data suggest that constitutive epithelial IKKβ activity in *Apc*$^{+/\Delta IEC}$ mice may increase tumor initiation by accelerating *Apc* allelic loss or by enhancing the survival or proliferation of cells that have undergone *Apc* loss.

To test whether constitutive epithelial NF-κB activity increases survival or proliferation of cells in premalignant lesions, we performed β-catenin, Ki67, and TUNEL staining on parallel paraffin sections of intestinal tissue from 6-wk-old *Ikkβ(EE)*^{IEC}*/Apc*$^{+/\Delta IEC}$ and *Apc*$^{+/\Delta IEC}$ mice. We could not detect any major differences in cell proliferation or apoptosis within tissue areas with activated β-catenin between the strains (Fig. S2 *D* and *E*).

***Ikkβ(EE)*^{IEC} Mice Show No Increase in β-Catenin Activation or Stem Cell Populations.** As NF-κB activation in IECs was suggested to accelerate intestinal tumorigenesis through synergistic cooperation with the β-catenin pathway (30), we examined nuclear β-catenin localization by immunohistochemistry (IHC) and cell

fractionation of intestinal crypt cells. Neither approach revealed increased amounts of nuclear β-catenin in *Ikkβ(EE)*^{IEC} mice (Fig. S3 *A* and *B*). Moreover, expression of key β-catenin target genes and stem cell markers was not elevated either (Fig. S3*C*). In situ hybridization for the stem cell marker OLFM4 (38) showed similar stem cell populations in WT and *Ikkβ(EE)*^{IEC} mice, but the proliferative compartment, as shown by staining with the Ki67 marker, was modestly increased in *Ikkβ(EE)*^{IEC} mice (Fig. S3*D*).

***Ikkβ(EE)*^{IEC} Mice Express High Amounts of iNOS and Markers of Nitrosative Stress.** Exploring mechanisms through which chronic IKKβ activation can influence intestinal tumor initiation, we reexamined the results of our previous transcriptomic analysis (31) and confirmed that expression of *Nos2* mRNA was highly up-regulated in IECs of *Ikkβ(EE)*^{IEC} mice: 80-fold in proximal SI villi and 7.8-fold in colonic crypts, following the *Villin* gene expression gradient (Fig. 2*A*). IHC of paraffin sections with an iNOS antibody revealed a substantial up-regulation of iNOS in *Ikkβ(EE)*^{IEC} mice, which was mostly visible on the apical side of the intestinal epithelium (Fig. 2*B*). Elevated iNOS expression in villi and crypts of *Ikkβ(EE)*^{IEC} mice was confirmed by immunoblot analysis (Fig. 2*C*). We also detected the NO• metabolite, nitrite, in plasma of *Ikkβ(EE)*^{IEC} mice and its concentrations were reduced upon administration of the partially selective iNOS inhibitor aminoguanidine (AG) (39) in the drinking water (Fig. S4*A*). Accordingly, nitrotyrosine, a marker for NO•-induced peroxynitrite formation, was elevated in the IECs of *Ikkβ(EE)*^{IEC} mice, as confirmed by blind scoring (Fig. S4*B*). To test whether iNOS expression was a direct result of NF-κB binding to the *Nos2* promoter, we performed chromatin immunoprecipitation (ChIP) analysis and detected p65/RelA binding to a known κB site at position -85; the p65 signal in the IECs of *Ikkβ(EE)*^{IEC} mice was twice as strong as the p65 signal in WT IECs (Fig. 2*D*). Collectively, these data suggest that activated NF-κB in the intestinal epithelium of *Ikkβ(EE)*^{IEC} mice directly up-regulates *Nos2* gene transcription, leading to elevated expression of iNOS protein and increased NO• production.

***Ikkβ(EE)*^{IEC} Intestinal Epithelium Is Subjected to Constitutive DNA Damage.** We hypothesized that chronic NO• production might lead to elevation of RNS in IECs, causing DNA damage and genotoxic stress. Indeed, we detected increased expression of phosphorylated histone 2AX, γ-H2AX, a marker for DNA double-strand breaks, in proximal SI and colonic crypts of *Ikkβ(EE)*^{IEC} mice by immunofluorescence staining of frozen intestinal sections and by immunoblot analysis (Fig. 3 *A* and *B*). Additionally, we analyzed DNA from the SI epithelium of WT and *Ikkβ(EE)*^{IEC} mice and using liquid-chromatography/tandem mass spectrometry found elevated amounts of 8,5′-cyclo-2′-deoxyadenosine (cdA) and 8,5′-cyclo-2′-deoxyguanosine (cdG) (40), which are oxidatively induced DNA lesions (41, 42), in *Ikkβ(EE)*^{IEC} mice (Fig. 3*C*). It is important to note that cdA and cdG are two of many endogenous reactive oxygen species (ROS)-induced DNA lesions. Furthermore, cdA and cdG are stable lesions and their formation is inhibited under aerobic conditions (42), rendering them unlikely to decompose or be artificially generated during DNA isolation and sample preparation. Thus, these lesions are valid and reliable markers for oxidative stress. Although cdA and cdG are considered substrates for nucleotide excision repair (43, 44), many oxidatively induced single-nucleobase lesions are substrates for base excision repair (BER). Along this line, we also found increased expression of apurinic/apyrimidinic endonuclease 1 (APE1), an enzyme involved in the BER pathway (Fig. S4 *C* and *D*) (45). The BER pathway repairs damaged bases, which may be caused by nitrosative and oxidative stress (46). These results indicate that *Ikkβ(EE)*^{IEC} intestinal epithelium is subjected to constitutive DNA damage and ongoing DNA repair.

Inhibition of iNOS Diminishes the IKKβ-Mediated Increase in Tumor Initiation. In view of the findings described above, we hypothesized that *Ikkβ(EE)*^{IEC} mice bearing a single *Apc* allele may be more prone to tumorigenesis because RNS-induced DNA damage in their IECs may lead to up-regulation of DNA recombination, as part of the global DNA damage response (47), and thereby enhance LOH. To examine this possibility, we treated mice with the iNOS inhibitor AG and analyzed them for tumor formation at 3 mo of age or for β-catenin^{+} premalignant foci at 6 wk of age. Both tumor number and tumor load, as well as the number of early β-catenin^{+} foci were reduced upon AG treatment of *Ikkβ(EE)*^{IEC}/*Apc*$^{+/\Delta IEC}$ mice (Fig. 4*A*). Consistently, we observed decreased γ-H2AX abundance after 2 wk of AG treatment in *Ikkβ(EE)*^{IEC} mice (Fig. 4 *B* and *C*), suggesting that NO• production may induce the accumulation of this DNA damage marker.

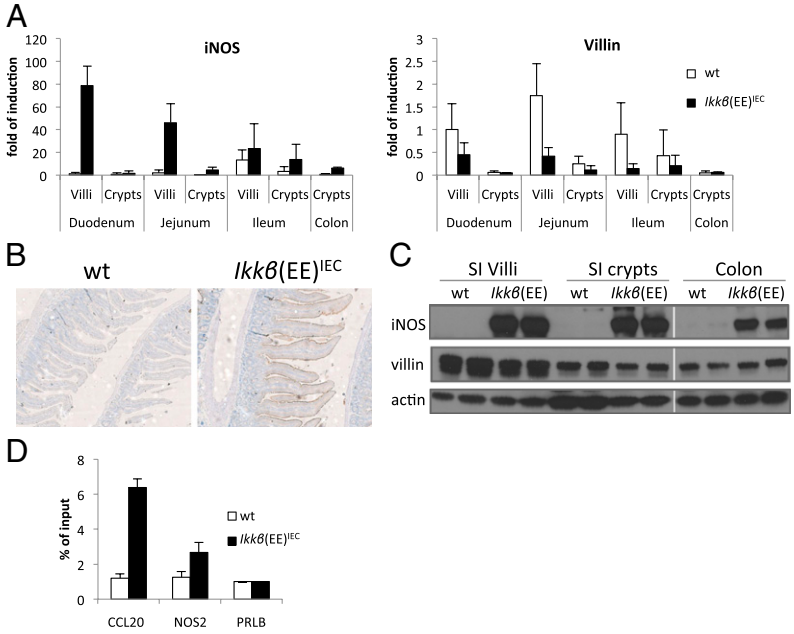

Fig. 2. iNOS is elevated in *Ikkβ(EE)*^{IEC} mice. (*A*) qRT-PCR of iNOS and Villin expression in various intestinal regions of 2-mo-old mice of the indicated genotypes. (*B*) IHC for iNOS performed on sections of SI of 2-mo-old mice. (*C*) Immunoblot analysis of iNOS expression in indicated intestinal regions of 2-mo-old mice. (*D*) ChIP analysis of p65/RelA recruitment to the indicated promoter regions performed on SI villi of 2-mo-old mice. The *Ccl20* (most up-regulated gene in *Ikkβ(EE)*^{IEC} mice) and *Prlb* promoters were used as positive and negative controls, respectively.

CELL BIOLOGY

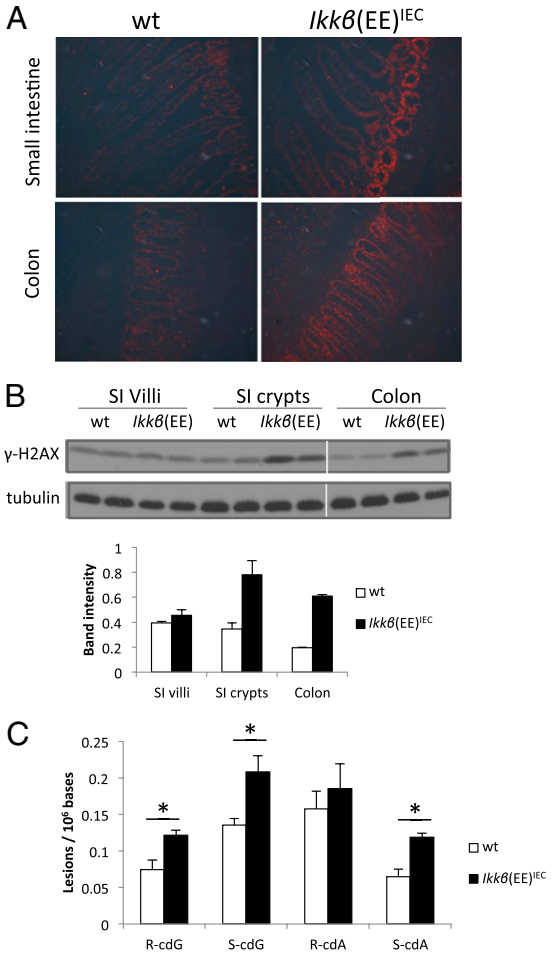

Fig. 3. DNA damage in *Ikkβ(EE)*^{IEC} mice. (*A*) Immunofluorescence analysis with anti–γ-H2AX antibody of frozen sections of intestinal tissue from 2-mo-old mice. (*B*) Immunoblot analysis γ-H2AX abundance in indicated intestinal regions of 2-mo-old mice. Shown are two mice per genotype with average band intensities indicated below. (*C*) Levels of 8,5′-cyclopurine-2′-deoxynucleosidesin mouse intestinal epithelium nuclear DNA (n = 3 for each genotype). cdG, 8,5′-cyclo-2′-deoxyguanosine; cdA, 8,5′-cyclo-2′-deoxyadenosine. R and S represent the 5′R and 5′S diastereoisomers, respectively.

Discussion

The role of inflammation in cancer development is well established and some underlying mechanisms were unraveled (3). Transient NF-κB activation in IECs, caused by inflammation, contributes to CAC tumorigenesis by inhibiting apoptosis in premalignant cells, whereas inflammatory NF-κB activation in lamina propria macrophages leads to production of growth factors and cytokines that stimulate the proliferation of premalignant cells (4). These and other results suggest that inflammation mainly affects tumor development at the tumor promotion stage (3). However, it was also proposed that persistent chronic inflammation can lead to induction of oncogenic mutations through ROS/RNS-dependent mechanisms (48), with more recent findings supporting this notion (10). Nonetheless, it has not been shown whether and how asymptomatic epithelial NF-κB activation, such as caused by local low-grade inflammatory processes, can affect tumor initiation rates.

Using mice that express a constitutively active form of IKKβ in IECs without active and tissue-destructive inflammation (31), we investigated whether persistent NF-κB activation can affect tumor initiation. We now show that activation of NF-κB in IECs induces spontaneous duodenal adenomas in aged mice. These tumors show no nuclear β-catenin activation, but express higher amounts of p53 without the associated up-regulation of p53 target genes. We therefore speculate that p53 may have been mutationally inactivated in these tumors. Although *Ikkβ(EE)*^{IEC} mice mainly develop duodenal tumors, they may represent a model for at least some aspects of human colitis-associated tumorigenesis, those that lead to *Tp53* mutations (12). Notably, p53 loss of function was suggested to be the tumor-initiating event in this type of cancer (49).

Our data also show that NF-κB activation in IECs of *Apc*$^{+/\Delta IEC}$ mice strongly enhances formation of colonic and SI adenomas by 3 mo of age and premalignant lesions containing activated β-catenin already at 4 wk of age. Tumors in *Apc*$^{+/\Delta IEC}$ mice are formed when some cells randomly loose the WT *Apc* allele, thereby allowing β-catenin activation and clonal expansion, similarly to the *Apc*$^{+/Min}$ model (50). Because IKKβ(EE)-driven NF-κB activation had no detectable effect on apoptosis of cells with activated β-catenin (Fig. S2*E*) or on β-catenin signaling in mice that retain APC expression (Fig. S3 *A–C*), we conclude that NF-κB activation in IECs of *Apc*$^{+/\Delta IEC}$ mice most likely enhances tumorigenesis by accelerating loss of the WT *Apc* allele, thereby leading to accelerated formation of β-catenin^{+} lesions. This conclusion is consistent with our inability to identify a measurable effect of NF-κB on IEC survival and the size of the crypt stem cell compartment in unchallenged mice, although NF-κB activation led to a modest increase in the size of the transit-amplifying compartment. Furthermore, *Ikkβ(EE)*^{IEC} mice do not exhibit any colitis or tissue destruction (31), further suggesting that less direct mechanisms of tumorigenesis, such as compensatory proliferation, are unlikely to be involved in this case of inflammation-driven tumor initiation.

Ikkβ(EE)^{IEC} mice expressed high amounts of iNOS in their IECs and displayed high levels of nitrosative and oxidative stress and DNA damage, which were diminished after treatment with the iNOS inhibitor AG. This treatment also decreased early β-catenin^{+} premalignant lesions and visible tumors, suggesting that elevated iNOS expression may be responsible for accelerated tumor initiation in these mice. Previous studies have already shown that inhibition of iNOS can attenuate formation of adenomas in *Apc*$^{+/Min}$ mice (21). However, the cause of iNOS up-regulation in these mice was neither identified nor was it demonstrated that iNOS expression activity led to DNA damage.

Another model of IEC-specific NF-κB activation was recently described, in which IKKβ-driven NF-κB was found to synergize with the β-catenin pathway and increase expression of stem cell markers (30). In this model, an IKKβ(EE) transgene was integrated into the *Rosa26* locus and was activated through Cre-recombinase–mediated excision of a STOP cassette, resulting in efficient expression of IKKβ(EE) in all IECs. By contrast, in our system the transgene itself is controlled by the *Villin* promoter and its expression level is directly proportional to that of Villin, such that it is expressed in higher amounts in the proximal SI than in the distant colon. Different patterns of transgene expression may explain why our mice only exhibit spontaneous tumors in the proximal SI and show no increase in stem cells markers. Nonetheless, the cause for tumor initiation in their *Ikk2(ca)*^{IEC} mice has not been identified, but given the large increase in iNOS expression seen in our *Ikkβ (EE)*^{IEC} mice, we presume that the *Ikk2(ca)*^{IEC} mice also express high amounts of iNOS and undergo nitrosative and oxidative stress, which contribute to tumor initiation.

Inflammation can contribute to tumorigenesis by various mechanisms (3). DNA damage induced by chronic inflammation was suggested to contribute to intestinal tumorigenesis in a mouse model of colitis based on repetitive dextran sodium sulfate administration (10). Also, iNOS was shown to contribute to colon cancer development in *Helicobacter hepaticus*-infected Rag2-deficient mice, where it is produced by infiltrating macrophages, although its roles in colitis and in cancer development were not dissected (51). Interestingly, these mice were recently found to exhibit certain DNA damage products in their colonic epithelium, associated with macrophage and neutrophil infiltration, which may underlie tumor development in this model (9).

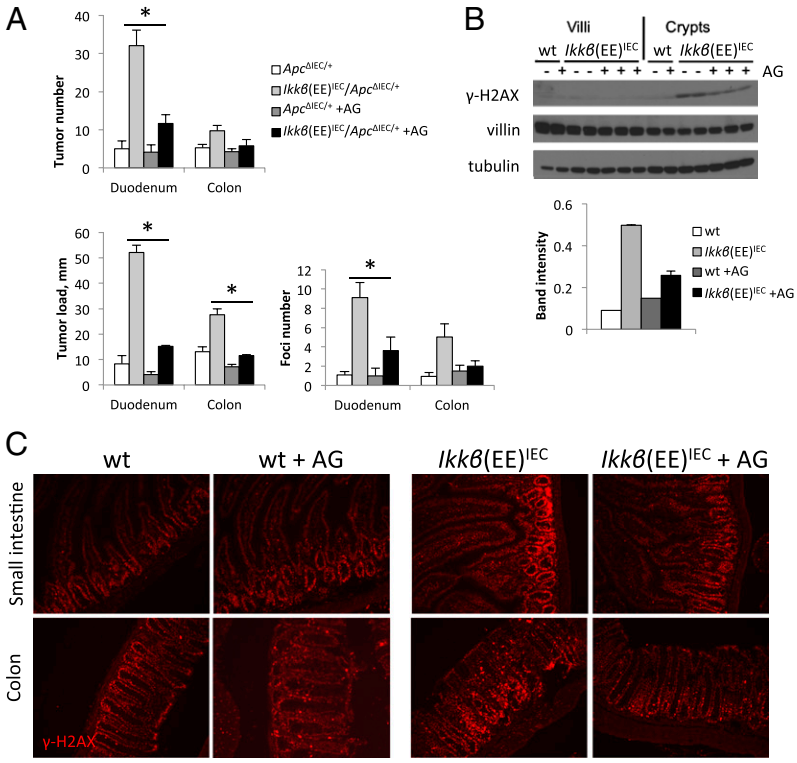

Fig. 4. AG treatment inhibits tumorigenesis in *Ikkβ(EE)*^{IEC}/*Apc*$^{+/\Delta IEC}$ mice. (*A*) Tumor number and tumor load were determined in 3-mo-old mice of indicated genotype ($n > 10$ per group); β-catenin$^+$ foci were determined in 6-wk-old mice ($n > 8$). AG mice were treated with 2 g/L of AG in drinking water starting at 4 wk of age. (*B*) Immunoblot analysis of γ-H2AX in SI villi and crypts of 2-mo-old mice untreated (–) or treated (+) with AG for 2 wk. Quantification of band intensity for crypts is shown. (*C*) Immunofluorescence analysis with γ-H2AX antibody of frozen sections of 2-mo-old WT and *Ikkβ(EE)*^{IEC} mice, untreated or treated with AG for 2 wk.

The role of NO• in promoting DNA damage was studied mostly in vitro, and the chemistry of its action on DNA is complex (52). NO•-derived ROS and RNS can cause single-strand breaks by attacking sugar moieties and can also create nucleobase modifications, such as deamination (52). During BER, modified nucleobases are removed by DNA glycosylases and DNA single-strand breaks are formed at abasic sites by AP endonucleases, such as APE1. These single-strand breaks are further repaired by downstream BER enzymes, but in cells engaged in DNA replication they can be converted into double-strand breaks (53). Consistently, we find increased amounts of γ-H2AX, a marker of double-strand DNA breaks, in crypts of *Ikkβ(EE)*^{IEC} mice. Because this constitutive increase in DNA damage appears to be tolerated, as only rare apoptotic cells are detected in unchallenged *Ikkβ(EE)*^{IEC} mice, it is likely that the NO•-exposed cells are engaged in DNA repair. A common way to repair double-strand DNA breaks is homologous recombination (47); generally a neutral process, it can also promote LOH in case of allelic mutation or deletion. Indeed, it was shown for *Apc*$^{+/Min}$ mice, that tumor initiation is caused by LOH induced by homologous recombination (54). Therefore, it is likely that NO• production in *Ikkβ(EE)*^{IEC} mice increases the rate of homologous recombination, leading to accelerated tumorigenesis when coupled with allelic *Apc* deletion. Indeed, NO• was shown to induce homologous recombination in cultured cells (55).

Collectively, our data strongly suggest that activated epithelial NF-κB can accelerate tumor initiation by up-regulation of iNOS, which induces DNA damage and elevates rates of LOH. These findings further illustrate how subclinical, low-grade, proinflammatory processes contribute to tumor initiation and suggest that iNOS inhibition may be a valid cancer preventive strategy.

Experimental Procedures

Mice and Tissue Analysis. All mice were on the C57BL/6 background. *Ikkβ(EE)*^{IEC} mice were previously described (31). *Villin*-Cre [B6.SJL-Tg(*vil*-Cre)997Gum/J] mice were obtained from The Jackson Laboratory. *Apc*$^{F/F}$ mice were from Eric R. Fearson (University of Michigan, Ann Arbor, MI). *Apc*$^{+/\Delta IEC}$ and *Apc*$^{+/\Delta IEC}$/*Ikkβ(EE)*^{IEC} mice were generated by crossing *Villin*-Cre females with *Apc*$^{F/F}$/*Ikkβ(EE)*^{IEC} males and selecting Cre$^+$ mice; *Ikkβ(EE)*^{IEC} transgene-positive and -negative mice were born in the expected Mendelian ratio. All mice were maintained in filter-topped cages on autoclaved food and water at University of California at San Diego (UCSD) according to National Institutes of Health (NIH) guidelines, and all experiments were performed in accordance with UCSD and NIH guidelines and regulations. For analysis, intestines were removed and divided into duodenum (6 most proximal centimeters), jejunum (the proximal half of the small intestine excluding duodenum), ileum (the distal half of the small intestine), and colon (all of the large intestine after cecum removal, including rectum); in other cases, the proximal 15 cm were analyzed collectively as "small intestine." Macroscopic tumors were counted and measured with a caliper. For nitrite analysis in plasma, retroorbital blood was collected and ultra-filtered (Amicon 10K filter; Millipore), and nitrite concentration was measured using a Griess reaction kit (Promega).

Histological Analysis. Intestines were flushed with ice-cold 10% neutral buffered formalin. Intestinal tissue was prepared as Swiss rolls, fixed in formalin for 24 h, and transferred to 70% (vol/vol) ethanol. Fixed tissue was embedded in paraffin and 5-μM sections were prepared and stained using standard immunohistochemistry procedures. The sections were boiled in citrate buffer for antigen retrieval and stained overnight with anti–β-catenin or anti-Ki67 antibodies (GenTex; 1:200 dilution for both). For immunofluorescence studies, tissues were frozen in optimal cutting temperature compound, cut on a cryomicrotome, air-dried, and fixed in 25% (vol/vol) methanol in acetone. The sections were incubated overnight with γ-H2AX antibody (Cell Signaling). TUNEL assay was performed using a in situ death detection TMR kit (Roche) on paraffin sections.

In Situ Hybridization. In situ hybridization was performed with OLFM4 probe as previously described (38).

iNOS, Nitrotyrosine, and APE1 Staining. Serial sections of intestinal tissues were incubated with antibodies against iNOS (160862; Cayman; 1:1,000), nitrotyrosine (N0409; Sigma 1:1,000), and APE-1 (NB100-101; Novus; 1:5,000). To ensure even staining and reproducible results, sections were incubated by slow rocking overnight in primary antibodies (4 °C) using the Antibody AmplifierTM (ProHisto). Then sections were processed using EnVision+ System-HRP kits (DakoCytomation) according to the manufacturer's protocols. The chromogen was 3,3′ diaminobenzidine and sections were counterstained with 1% methyl green. Intensity and degree of staining were evaluated independently by two blinded investigators. For each tissue section, the percentage

of positive cells was scored on a scale of 0–5 for the percentage of tissue stained: 0 (0% positive cells), 1 (<10%), 2 (11–25%), 3 (26–50%), 4 (51–80%), and 5 (80%). Staining intensity was scored on a scale of 0–3. The two scores were multiplied, resulting in an immunoreactivity score (IRS) ranging from 0 to 15. Average was taken from two slides analyzed for each sample.

IEC Isolation, qRT-PCR, and Immunoblot Analysis. Intestines were removed, flushed with ice-cold PBS, and opened longitudinally on ice. For the small intestine, villi were removed by gentle scraping with a spatula, spun down in PBS at 300 × *g*, and snap frozen. The intestines were cut into 5-mm pieces, washed briefly with PBS, and placed into PBS supplemented with 20 mM EDTA and protease and phosphatase inhibitors. The tissue was vortexed for 20 min at 4 °C and passed through a 70-μm strainer; the resulting single crypts and cells were spun down at 300 × *g* and snap frozen. For qRT-PCR, RNA was isolated with RNeasy kit (Qiagen), converted into cDNA with reverse transcriptase (Biorad), and analyzed via qPCR with primers from qPrimerDepot, using the Hprt gene for normalization. For immunoblot analysis, cells were lysed in 1% SDS buffer and analyzed for protein content by a bicinchoninic acid assay. Cytoplasmic and nuclear extracts were obtained as previously described (31). Proteins were separated by SDS/PAGE and transferred to nitrocellulose membranes that were incubated with antibodies against iNOS (sc-8310), villin (sc-7672), APE1 (sc-55498; all three from Santa Cruz), actin (Sigma; A4700), tubulin (Sigma; T5168), γ-H2AX (Cell Signaling; 9718), acetylated histone H3 (Upstate; 06–599), p53 (Cell Signaling; 2524) and β-catenin (GeneTex; GTX61089).

ChIP Analysis. Epithelium from small intestine was scraped into 1% formaldehyde in PBS and fixed for 10 min at room temperature. Chromatin was precipitated with a p65 antibody (Santa Cruz; sc-372) as previously described (31). Precipitated material and input DNA were analyzed by qPCR and percentage of input was calculated and normalized to nonspecific DNA region (*Prlb* gene promoter). Primer sequences are available upon request.

Oxidative DNA Lesion Analysis. DNA was extracted from intestinal villi and analyzed as previously described (40).

Statistical Analysis. Throughout the manuscript, error bars represent SEM between samples from separate mice. *P* values of 0.05 or less are considered significant.

ACKNOWLEDGMENTS. This work was supported by National Institutes of Health Grants AI043477 (to M.K.) and CA101864 (to Y.W.), William K. Warren Foundation Grant DK035108 (to M.K.), and the Strategic Young Researcher Overseas Visits Program for Accelerating Brain Circulation (K.T.).

1. Jemal A, Siegel R, Xu J, Ward E (2010) Cancer statistics, 2010. *CA Cancer J Clin* 60: 277–300.
2. Hardy RG, Meltzer SJ, Jankowski JA (2000) ABC of colorectal cancer. Molecular basis for risk factors. *BMJ* 321:886–889.
3. Grivennikov SI, Greten FR, Karin M (2010) Immunity, inflammation, and cancer. *Cell* 140:883–899.
4. Greten FR, et al. (2004) IKKbeta links inflammation and tumorigenesis in a mouse model of colitis-associated cancer. *Cell* 118:285–296.
5. Pikarsky E, et al. (2004) NF-kappaB functions as a tumour promoter in inflammation-associated cancer. *Nature* 431:461–466.
6. Garrett WS, et al. (2009) Colitis-associated colorectal cancer driven by T-bet deficiency in dendritic cells. *Cancer Cell* 16:208–219.
7. Erdman SE, et al. (2003) CD4+ CD25+ regulatory T lymphocytes inhibit microbially induced colon cancer in Rag2-deficient mice. *Am J Pathol* 162:691–702.
8. Okayasu I, et al. (2002) Dysplasia and carcinoma development in a repeated dextran sulfate sodium-induced colitis model. *J Gastroenterol Hepatol* 17:1078–1083.
9. Mangerich A, et al. (2012) Infection-induced colitis in mice causes dynamic and tissue-specific changes in stress response and DNA damage leading to colon cancer. *Proc Natl Acad Sci USA* 109:E1820–E1829.
10. Meira LB, et al. (2008) DNA damage induced by chronic inflammation contributes to colon carcinogenesis in mice. *J Clin Invest* 118:2516–2525.
11. D'Incà R, et al. (2004) Oxidative DNA damage in the mucosa of ulcerative colitis increases with disease duration and dysplasia. *Inflamm Bowel Dis* 10:23–27.
12. Hussain SP, et al. (2000) Increased p53 mutation load in noncancerous colon tissue from ulcerative colitis: A cancer-prone chronic inflammatory disease. *Cancer Res* 60:3333–3337.
13. de la Chapelle A (2004) Genetic predisposition to colorectal cancer. *Nat Rev Cancer* 4: 769–780.
14. Powell SM, et al. (1992) APC mutations occur early during colorectal tumorigenesis. *Nature* 359:235–237.
15. Fearnhead NS, Britton MP, Bodmer WF (2001) The ABC of APC. *Hum Mol Genet* 10: 721–733.
16. Morin PJ, et al. (1997) Activation of beta-catenin-Tcf signaling in colon cancer by mutations in beta-catenin or APC. *Science* 275:1787–1790.
17. Gupta RA, Dubois RN (2001) Colorectal cancer prevention and treatment by inhibition of cyclooxygenase-2. *Nat Rev Cancer* 1:11–21.
18. Rothwell PM, et al. (2011) Effect of daily aspirin on long-term risk of death due to cancer: Analysis of individual patient data from randomised trials. *Lancet* 377:31–41.
19. Rothwell PM, et al. (2010) Long-term effect of aspirin on colorectal cancer incidence and mortality: 20-year follow-up of five randomised trials. *Lancet* 376:1741–1750.
20. Oshima M, et al. (1996) Suppression of intestinal polyposis in Apc delta716 knockout mice by inhibition of cyclooxygenase 2 (COX-2). *Cell* 87:803–809.
21. Ahn B, Ohshima H (2001) Suppression of intestinal polyposis in Apc(Min/+) mice by inhibiting nitric oxide production. *Cancer Res* 61:8357–8360.
22. Kohno H, et al. (2007) A specific inducible nitric oxide synthase inhibitor, ONO-1714 attenuates inflammation-related large bowel carcinogenesis in male Apc(Min/+) mice. *Int J Cancer* 121(3):506–513.
23. MacMicking J, Xie QW, Nathan C (1997) Nitric oxide and macrophage function. *Annu Rev Immunol* 15:323–350.
24. Beck PL, et al. (2004) Paradoxical roles of different nitric oxide synthase isoforms in colonic injury. *Am J Physiol Gastrointest Liver Physiol* 286:G137–G147.
25. Kolios G, Valatas V, Ward SG (2004) Nitric oxide in inflammatory bowel disease: A universal messenger in an unsolved puzzle. *Immunology* 113:427–437.
26. Hoffman RA, et al. (1997) Constitutive expression of inducible nitric oxide synthase in the mouse ileal mucosa. *Am J Physiol* 272:G383–G392.
27. Karin M (2006) Nuclear factor-kappaB in cancer development and progression. *Nature* 441:431–436.
28. Ben-Neriah Y, Karin M (2011) Inflammation meets cancer, with NF-κB as the matchmaker. *Nat Immunol* 12:715–723.
29. Häcker H, Karin M (2006) Regulation and function of IKK and IKK-related kinases. *Sci STKE* 2006:re13.
30. Vlantis K, et al. (2011) Constitutive IKK2 activation in intestinal epithelial cells induces intestinal tumors in mice. *J Clin Invest* 121:2781–2793.
31. Guma M, et al. (2011) Constitutive intestinal NF-κB does not trigger destructive inflammation unless accompanied by MAPK activation. *J Exp Med* 208:1889–1900.
32. Blache P, et al. (2004) SOX9 is an intestine crypt transcription factor, is regulated by the Wnt pathway, and represses the CDX2 and MUC2 genes. *J Cell Biol* 166:37–47.
33. Matheu A, et al. (2012) Oncogenicity of the developmental transcription factor Sox9. *Cancer Res* 72:1301–1315.
34. Sansom OJ, et al. (2007) Myc deletion rescues Apc deficiency in the small intestine. *Nature* 446:676–679.
35. Muncan V, et al. (2006) Rapid loss of intestinal crypts upon conditional deletion of the Wnt/Tcf-4 target gene c-Myc. *Mol Cell Biol* 26:8418–8426.
36. Hinoi T, et al. (2007) Mouse model of colonic adenoma-carcinoma progression based on somatic Apc inactivation. *Cancer Res* 67:9721–9730.
37. Neufert C, Becker C, Neurath MF (2007) An inducible mouse model of colon carcinogenesis for the analysis of sporadic and inflammation-driven tumor progression. *Nat Protoc* 2:1998–2004.
38. van der Flier LG, et al. (2009) Transcription factor achaete scute-like 2 controls intestinal stem cell fate. *Cell* 136:903–912.
39. Alderton WK, Cooper CE, Knowles RG (2001) Nitric oxide synthases: Structure, function and inhibition. *Biochem J* 357:593–615.
40. Wang J, et al. (2011) Quantification of oxidative DNA lesions in tissues of Long-Evans Cinnamon rats by capillary high-performance liquid chromatography-tandem mass spectrometry coupled with stable isotope-dilution method. *Anal Chem* 83:2201–2209.
41. Wang Y (2008) Bulky DNA lesions induced by reactive oxygen species. *Chem Res Toxicol* 21:276–281.
42. Jaruga P, Dizdaroglu M (2008) 8,5′-Cyclopurine-2′-deoxynucleosides in DNA: mechanisms of formation, measurement, repair and biological effects. *DNA Repair (Amst)* 7: 1413–1425.
43. Brooks PJ, et al. (2000) The oxidative DNA lesion 8,5′-(S)-cyclo-2′-deoxyadenosine is repaired by the nucleotide excision repair pathway and blocks gene expression in mammalian cells. *J Biol Chem* 275:22355–22362.
44. Kuraoka I, et al. (2000) Removal of oxygen free-radical-induced 5′,8-purine cyclodeoxynucleosides from DNA by the nucleotide excision-repair pathway in human cells. *Proc Natl Acad Sci USA* 97:3832–3837.
45. Sung JS, Demple B (2006) Roles of base excision repair subpathways in correcting oxidized abasic sites in DNA. *FEBS J* 273:1620–1629.
46. Kow YW (2002) Repair of deaminated bases in DNA. *Free Radic Biol Med* 33:886–893.
47. Helleday T, Lo J, van Gent DC, Engelward BP (2007) DNA double-strand break repair: From mechanistic understanding to cancer treatment. *DNA Repair (Amst)* 6:923–935.
48. Hussain SP, Hofseth LJ, Harris CC (2003) Radical causes of cancer. *Nat Rev Cancer* 3:276–285.
49. Yin J, et al. (1993) p53 point mutations in dysplastic and cancerous ulcerative colitis lesions. *Gastroenterology* 104:1633–1639.
50. Luongo C, Moser AR, Gledhill S, Dove WF (1994) Loss of Apc+ in intestinal adenomas from Min mice. *Cancer Res* 54:5947–5952.
51. Erdman SE, et al. (2009) Nitric oxide and TNF-alpha trigger colonic inflammation and carcinogenesis in *Helicobacter hepaticus*-infected, Rag2-deficient mice. *Proc Natl Acad Sci USA* 106:1027–1032.
52. Burney S, Caulfield JL, Niles JC, Wishnok JS, Tannenbaum SR (1999) The chemistry of DNA damage from nitric oxide and peroxynitrite. *Mutat Res* 424:37–49.
53. Kuzminov A (2001) Single-strand interruptions in replicating chromosomes cause double-strand breaks. *Proc Natl Acad Sci USA* 98:8241–8246.
54. Haigis KM, Dove WF (2003) A Robertsonian translocation suppresses a somatic recombination pathway to loss of heterozygosity. *Nat Genet* 33:33–39.
55. Kiziltepe T, et al. (2005) Delineation of the chemical pathways underlying nitric oxide-induced homologous recombination in mammalian cells. *Chem Biol* 12:357–369.